Journal of Arid Environments 207 (2022) 104848

Contents lists available at ScienceDirect

Journal of Arid Environments

journal homepage: www.elsevier.com/locate/jaridenv

Geomorphology of sand dunes in the Taklamakan Desert based on ERA5 reanalysis data

Wentao Sun [a,b], Xin Gao [a,b,*]

[a] State Key Laboratory of Desert and Oasis Ecology, Xinjiang Institute of Ecology and Geography, Chinese Academy of Sciences, 818 South Beijing Road, Urumqi, 830011, Xinjiang, China
[b] University of Chinese Academy of Sciences, Beijing, 100049, China

ARTICLE INFO

Keywords:
Dunes
ERA5 reanalysis data
Wind regime
Bed instability mode
Elongation mode
Taklamakan Desert

ABSTRACT

The characteristics of the wind regime and the development of dune morphology in the Taklamakan Desert have been the focus of scholars. In this study, we used ERA5 reanalysis wind data at a height of 10 m from 1979 to 2019 to examine the sand transport and wind regime characteristics of the entire Taklamakan Desert. We combined the two latest dune development modes, i.e., bed instability and elongation modes, and determined that: (1) Taklamakan Desert is overall characterized by a lower wind energy environment; the wind and sand activity intensities are highest in the eastern part of the desert, with a decreasing trend from the east to the west. The wind direction in the eastern region shows unimodal characteristics due to the backward easterly wind; the wind regime gradually becomes complicated from the northeast to the southwest; (2) the morphological alignments of dunes can be predicted by such modern wind regimes combined with the latest dune development modes. Large longitudinal dunes in the middle of the desert can be predicted with the elongation mode, whereas secondary transverse dunes, which derive from these composite dunes, can be predicted using the bed instability mode. Collectively, this paper fills the gap of the lack of uniform and standardized macro-scale wind data in the Taklamakan Desert, and the two modes of dune development derived from ERA5 reanalysis data can match the morphology and trend of most modern dunes.

1. Introduction

1.1. Dune classification

The formation and development processes of sand dunes have been the focus of research in sandy landscapes because they are an important aeolian geomorphological feature (Bagnold, 1941; Pye and Tsoar, 1990; Charru et al., 2014). Dunes form from certain sand sources, under effective wind regimes, and suitable timing concerning sand transport and accumulation (Bagnold, 1941; Pye and Tsoar, 1990). The spatial and temporal variability in the wind and subsurface conditions influence their types.

There are different classification criteria for dune morphology and orientation. Based on the wind regime and sand availability, dunes can be classified into the following basic forms (Wasson and Hyde, 1983, Fig. 1): 1) barchan dunes, which generally form in areas with a finite supply of sand and a unidirectional wind regime; 2) barchan dune chains or transverse dunes that form in areas with freely available sand under the same wind regime; and 3) pyramid dunes (star dunes) that generally form in areas with complex wind regimes and sufficient sand sources. 4) Large-scale longitudinal dunes develop only where sand sources are abundant (Courrech du Pont et al., 2014). The angle between the sand ridge-line of the longitudinal dune and the resultant drift direction is less than 15°. 5) Shadow dunes develop on the lee slopes of obstacles such as bushes, grasses, rocks and nebkhas, and are one of the main aeolian dunes on Earth and other planets (Bagnold, 1941; Hesp, 1981; Gunatilaka and Mwango, 1989; Mottola et al., 2015; Xiao et al., 2015; Hesp and Smyth, 2017; Yang et al., 2019; Zhao et al., 2019, 2021). They are likely to be observed in conditions of high wind direction variability and low sand supply. 6) Network dunes are generally formed under two nearly vertical wind regimes, with the main wind shaping the main beam and the vertical secondary wind shaping the secondary beam (Ping et al.,

Abbreviations: DP, Drift Potential; *RDP*, Resultant Drift Potential.

* Corresponding author. State Key Laboratory of Desert and Oasis Ecology, Xinjiang Institute of Ecology and Geography, Chinese Academy of Sciences, 818 South Beijing Road, Urumqi, 830011, Xinjiang, China.
E-mail address: gaoxin@ms.xjb.ac.cn (X. Gao).

https://doi.org/10.1016/j.jaridenv.2022.104848
Received 7 March 2022; Received in revised form 19 August 2022; Accepted 20 August 2022
Available online 30 August 2022

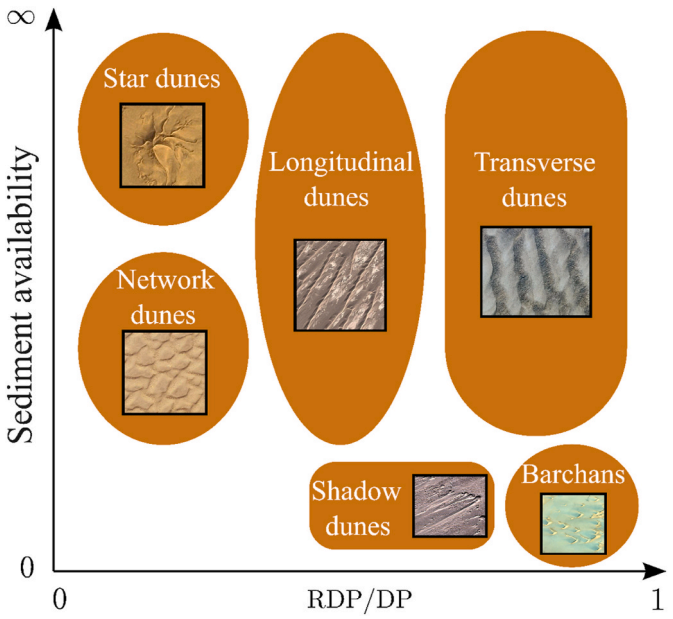

Fig. 1. Sand dune classification is based on the abundance of the sand source and wind complexity (Modified from Wasson and Hyde, 1983). *RDP/DP* is the ratio of resultant drift potential to drift potential, which reflects the complexity of wind direction variation.

2014), and there are deep sand nests between dunes. Linear dunes develop under bimodal or more complex wind regimes (Pye and Tsoar, 1990); their sand ridgelines are oriented in nearly the same direction as the resultant drift direction. However, researchers have found that linear dunes are also formed in many places under the action of unidirectional wind, especially when blocked by nebkhas because of the deflection flow on the crest of longitudinal (Zhou et al., 2020). In Wasson and Hyde's classification criteria, wind intensity and the role of vegetation were not considered.

Sand dunes can also be classified based on their orientation; considering the angle, φ, between the resultant drift potential and the dune ridgeline, they can be classified as transverse dunes ($\varphi \geq 75^{\circ}$), oblique dunes ($15^{\circ} < \varphi < 75^{\circ}$), and longitudinal dunes ($\varphi \leq 15^{\circ}$) (Hunter et al., 1983). Barchan dunes are simple transverse dunes with dune ridges approximately perpendicular to the resultant drift direction. Pyramid dunes (star dunes) have more than three sand ridgelines with no exact alignment (Zhang et al., 2012) and thus cannot be classified according to dune alignment. For linear dunes, studies have reported that their orientation is not merely parallel to the resultant drift direction (Livingstone and Warren, 1996; Lancaster, 2010; Courrech du Pont et al., 2014; Gao et al., 2015), therefore, linear dunes can be either longitudinal or oblique.

1.2. Sand dune development mechanisms

The formation and development mechanisms and morphological characteristics of dunes, particularly simple dunes, have been studied globally; however, conducting advanced studies on complex dunes has remained difficult owing to the complexity and diversity of study areas and limitations associated with observational technology.

As a basic component of aeolian geomorphology, various factors, including topography, wind regimes, and climate, influence dune morphology and orientation. Based on the complex and diverse dune types, many sand dunes development patterns have been generated, such as wind erosion, accretion, deposition, and the evolution of simple to complex dunes (Bagnold, 1941; McKee, 1982; Tsoar, 1984; Pye and Tsoar, 1990; Livingstone and Warren, 1996; Bristow et al., 2000; Wang et al., 2004; Dong et al., 2009; Rubin, 2012; Zhang et al., 2012; Gao et al., 2015). The crest-normal net sand transport mechanism is derived from Rubin and Hunter (1987), which is a significant breakthrough in understanding the relationships between bedform orientation and flow pattern. As reported by Gao et al. (2015), when considering a bidirectional flow regime, they experimentally showed that sediment bedforms select the orientation for which the sum of the normal to crest components of the two transport vectors reaches its maximum value. Thus, they introduced the gross bedform-normal transport rule, which can be generalized to multidirectional flow patterns (Werner and Kocurek, 1997; Ping et al., 2014; Gao et al., 2015). Based on such rule together with the dune type classification, Courrech du Pont et al. (2014) proposed two dune development modes through underwater experiments, remote sensing image verification and theoretical analysis. They have demonstrated that there are two modes for dune orientation depending on sand availability. Each mode is associated with a specific dune growth mechanism. For periodic bidirectional wind regimes and two different conditions of sand availability, Gao et al. (2015) documented all the possible dune morphologies and orientations in the numerical

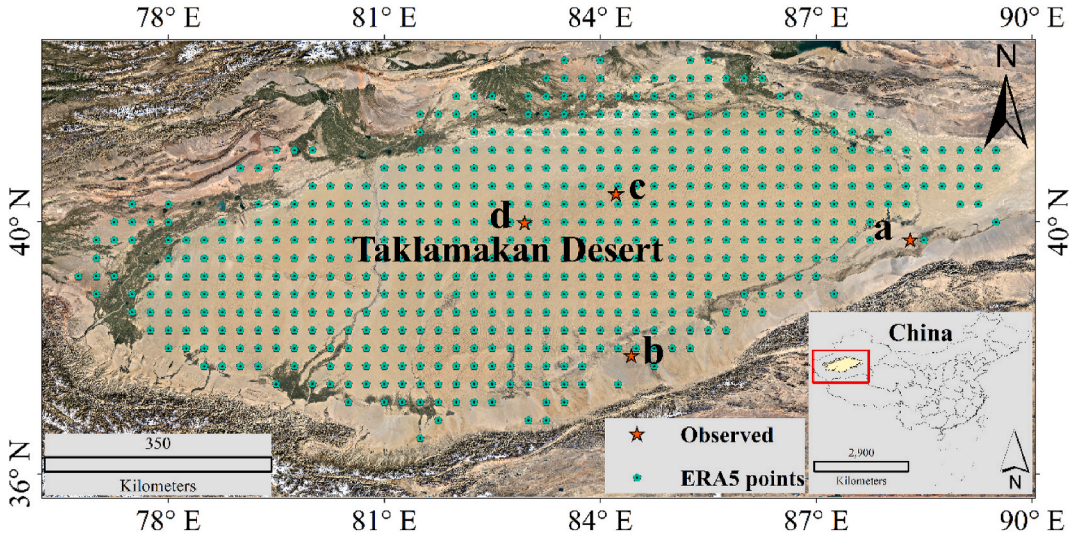

Fig. 2. Location of Taklamakan Desert. Sample site distribution of the selected ERA5 data (temporal resolution: 1 h; spatial resolution: 0.25° × 0.25°) in Taklamakan Desert. a, b, c, and d represent the weather stations we selected in the desert. Blue points represent the ERA5 data points while orange stars represent the locations of the weather stations. (For interpretation of the references to colour in this figure legend, the reader is referred to the Web version of this article.)

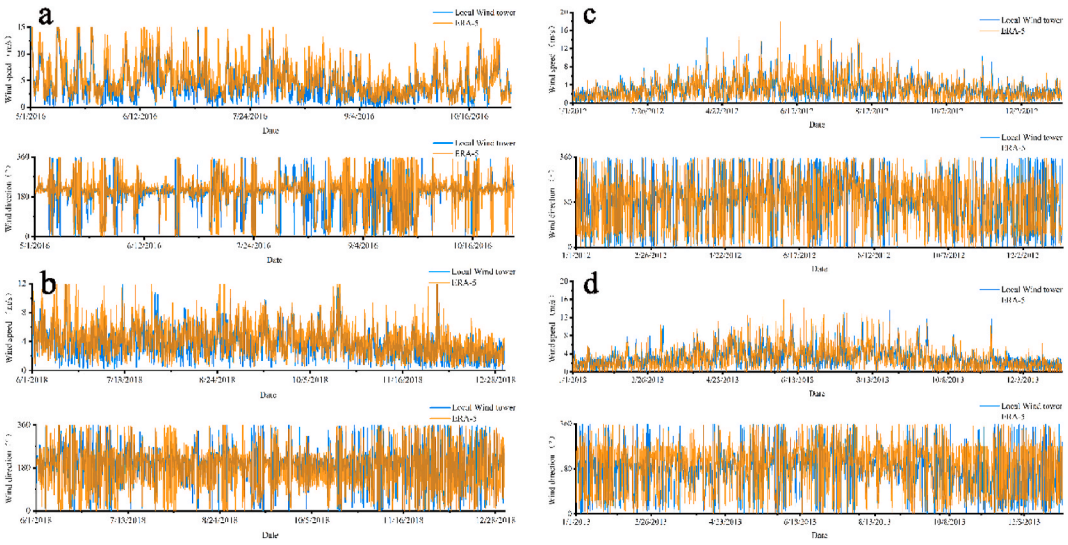

Fig. 3. Verification of the ERA5 reanalysis wind data accuracy. Panels a, b, c and d show the comparison of wind direction and speed from the observation station data and the ERA5 reanalysis data, respectively.

model.

Through indoor experiments and numerical simulation, it is shown that identical wind regimes can produce dunes with different orientations (Taniguchi et al., 2012; Parteli et al., 2014). The dune orientation under both development modes is defined by the angle between the sand ridge orientation and resultant drift direction. The angle of the bimodal wind regime and sand transport ratio affect the final dune orientation (Rubin and Hunter, 1987; Gao et al., 2015). Courrech du Pont et al. (2014) established a theoretical equation that describes the dune orientation as a function of the divergence angle of the wind regime. In this study, we analyzed the dune types in the Taklamakan Desert based on this theoretical mechanism.

1.3. Taklamakan status

Taklamakan Desert (known as the "dry pole" of the world), located in the Tarim Basin in Xinjiang, China, is the largest desert in China (Fig. 2) and the second-largest mobile desert worldwide (Zhu, 1980), with an area of 34×10^4 km^2 (Sun et al., 2009). The dune types in Taklamakan Desert are complex and diverse, ranging from simple dunes to complex/compound dunes. Their sandy landscapes and wind regimes have been the focus of recent studies. Owing to traffic restrictions and a lack of updated technology, studies on the Taklamakan Desert are limited compared with other global sand seas (Wang et al., 2002). Since the 1960s, scholars have examined the formation and movement of sand dunes along desert margins, such as in the southwest region (Zhu, 1964), drifting sand along desert roads (Dong et al., 2000), and sand transport wind characteristics (Chen et al., 1995). More recently, studies have been conducted on the wind regime and dune formation in the northeastern part of the desert (Wang et al., 2002). Some scholars also studied the near-surface wind regime in the Taklamakan Desert by using the data of meteorological stations (Zu et al., 2008). Including the influence of vegetation and temperature on surface wind speed (Liu et al., 2022). Some scholars have also studied wind erosion events in Tarim Basin under different wind speed levels (Zhou et al., 2020). However, with the development of reanalysis data, analyzing the wind regime and sand transport across the entire desert has become possible.

1.4. Research purpose

Using ERA5 reanalysis data, this study aims to analyze the characteristics of the wind regime and sand transport across Taklamakan Desert to effectively predict the dune morphology and orientation based on calculations of two dune development modes (bed instability mode and elongation mode) and verify whether the near-surface wind regime can explain the morphology and orientation of the modern dune types in Taklamakan Desert.

2. Methods

2.1. Dataset

The European Center for Medium-Range Weather Forecasts (ECWMF) was one of the earliest institutions to perform data reanalysis (https://www.ecmwf.int/). ERA5 is produced using 4D-Var data assimilation and model forecasts in CY41R2 of the ECMWF Integrated Forecast System (IFS), with 137 hybrid sigma/pressure (model) levels in the vertical and the top level at 0.01 hPa. Jon Olauson (2018) compared the modelling performance of ERA5 and MERRA-2 reanalysis data and found that ERA5 data had a higher correlation and the distribution and variation of hourly data were closer to the measured data. Meng et al. (2018) compared the data of 10 observation stations in Shandong, China and surrounding areas with ERA5 and ERA-Interim reanalysis data, and found that the assimilation data had a good correlation with the measured data. ERA5 data are more applicable than ERA-Interim data. Therefore, we selected ERA5 wind data (1979–2019) with a height of 10 m, a spatial resolution of 1 h, and a horizontal resolution of $0.25^\circ \times 0.25^\circ$ (Fig. 2) to calculate the corresponding wind-sand parameters.

In addition, remote sensing images, such as Google Earth satellite images, and measured weather data from four weather stations in the Taklamakan Desert were used in this study.

2.2. Verification of ERA5 data accuracy

To evaluate the accuracy of the ERA5 reanalysis data, the data were compared with measured data from four meteorological stations in the eastern (39.25° N, 88.31° E), southeastern (37.65° N, 84.43° E) and middle (39.49° N, 82.95° E; 39.89° N, 84.22° E) of Taklamakan Desert. This is because some dates are missing from the measured weather dataset as well as because of the presence of certain singular values within the dataset. Therefore, we selected wind data from a continuous time series of weather stations in the east (from January 05, 2016 to 10/31/2016), southeast (from January 06, 2018 to 12/31/2018) and middle (from January 01, 2012 to 12/31/2012; from January 01, 2013

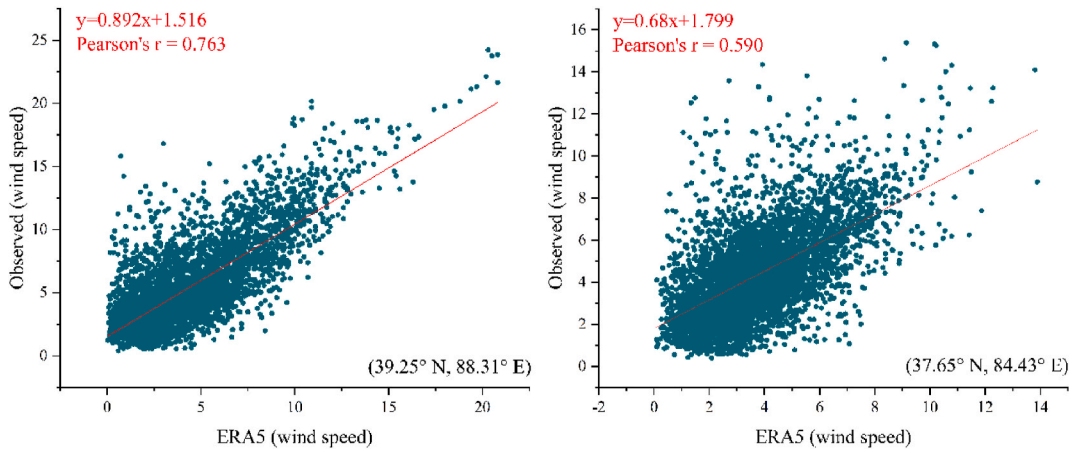

Fig. 4. Spatial analysis of assimilated data correlations for ERA5 and Observed datasets. Two weather stations in Fig. 2 (a and b).

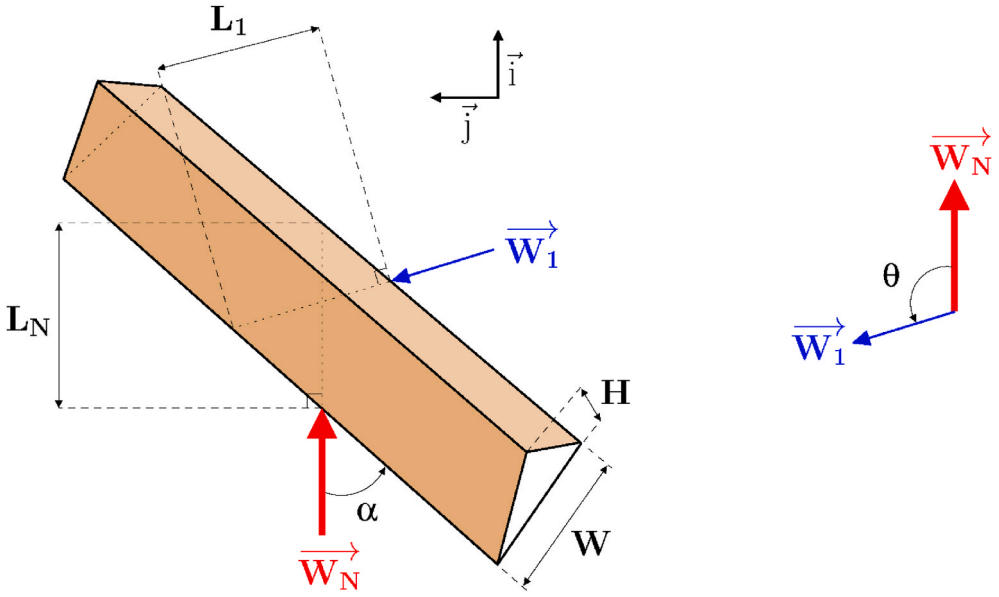

Fig. 5. Sketch of a linear dune submitted to a bimodal wind regime. Reproduced from Gao et al. (2015).

to 12/31/2013) (Fig. 3).

We have plotted the scatter-plot with correlation coefficients to compare the local measured wind data and the ERA5 wind data (Fig. 4). We found a high correlation between ERA5 data and weather station data, through wind speed frequency plots and scatter plots with correlation coefficients. Therefore, the above evidence could verify and support our results to some extent.

In general, the assimilated data were consistent with the measured data, demonstrating that the ERA5 data can be used to calculate the wind regime and sand transport characteristic parameters.

2.3. Wind regime

Here, we only used the complete time series from the 10-m wind data for the latitudinal and longitudinal components.

According to the ERA5 dataset, we calculated the wind speed, u_i, and direction, $\overrightarrow{x_i}$, at different times, $t_1 \leq t_i \leq t_{N_{obs}}$, iε[1; N_{obs}]. For each time step i, we computed the shear velocity as follows:

$$u_*^i = \frac{u_i k}{\log(z/z_0)}, \tag{1}$$

where z = 10 m is the height of the measured wind data, $z_0 = 10^{-3}$ m is the characteristic surface roughness (Courrech du Pont et al., 2014), and $k = 0.4$ is the von Karman constant. The value of the roughness z_0 depends on u_* as, in transport conditions, z_0 is controlled by the transport layer thickness. The threshold velocity u_{*c} for motion inception can be determined using the formula of Iversen and Rasmussen (1999):

$$u_{*c} = 0.1\sqrt{\frac{\rho_s}{\rho_f} gd} \tag{2}$$

where the gravitational acceleration, g, is 9.81 ms^{-2}, $\rho_s = 2.55 \times 10^3$ kg/m^3, $\rho_f = 1.293 \times 10^3$ kg/m^3, and the grain diameter, d, is 180 μm. These parameters are generally the global average values. In a given scope, resultant drift direction (*RDD*) is less dependent on the grain size and aerodynamic roughness. We selected the global average grain diameter. The sand-driving wind speed, $u_{*c} \approx 0.19$ ms^{-1}.

Many sand transport relationships have been obtained via wind-tunnel experiments, both analytical and phenomenological (Bagnold, 1941; Owen, 1964; Lettau and Lettau, 1978; Ungar and Haff, 1987; Iversen and Rasmussen, 1999; Andreotti, 2004; Sørensen, 2004; Durán and Herrmann, 2006; Durán et al., 2011; Sherman and Li, 2012; Pähtz et al., 2019; Wang et al., 2020). After a series of tests, Ungar and Haff

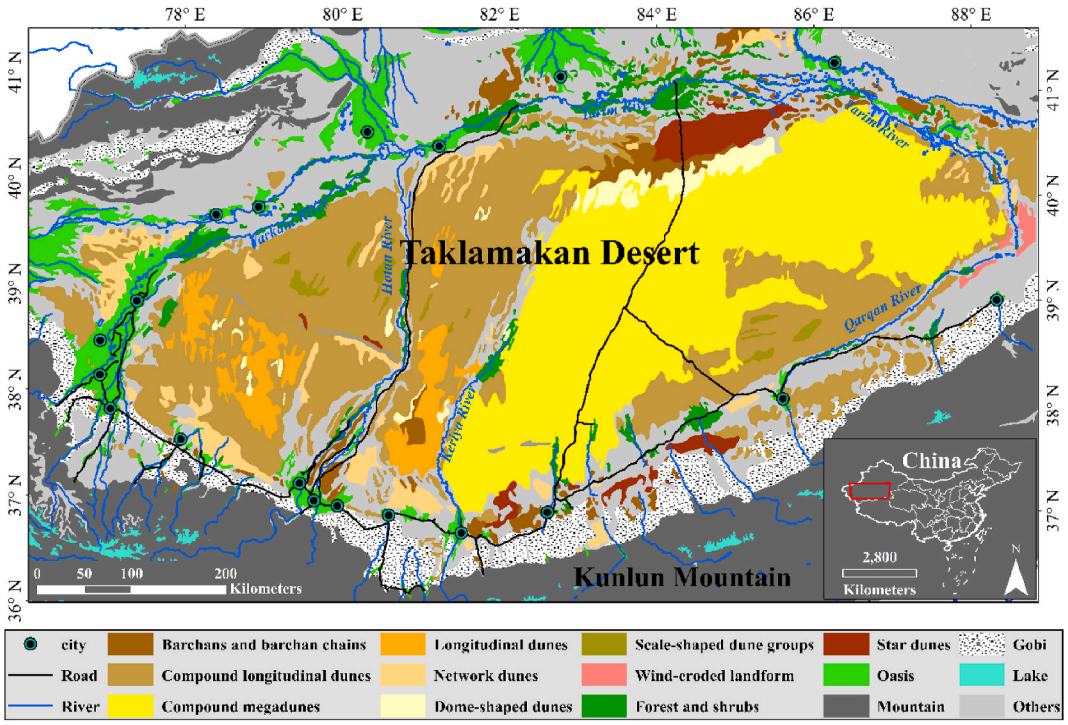

Fig. 6. Distribution of different dune types in Taklamakan Desert in 1978. The data are from Tibetan Plateau Data Center, https://doi.org/10.3972/westdc.008.2013.db. CSTR: 18406.11.westdc.008.2013.db. We reproduced the figure.

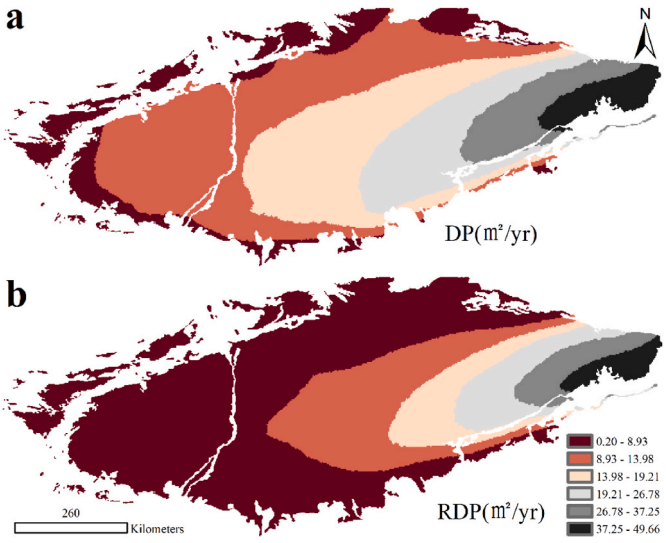

Fig. 7. Distribution of the drift potential (*DP*) and resultant drift potential (*RDP*) in Taklamakan Desert from 1979 to 2019. Based on the ERA5 wind data at a height of 10 *m*, the normal Kriging interpolation method is used to generate the continuous graph. The *DP* and *RDP* are in m^2/yr.

(1987) proposed such a relationship:

$$Q = 25\frac{\rho_f}{\rho_S}\sqrt{\frac{d}{g}}\left(u_*^2 - u_{*_c}^2\right), \tag{3}$$

where g is the acceleration due to gravity, d is the grain size, ρ_s is the density of sand, and ρ_f is the density of air. Equation (3) is used to calculate Q, the sediment transport per unit length of a saturated volume.

Next, we calculated the saturated sand flux on a flat sand bed for each time step:

$$\overrightarrow{Q_i} = \begin{cases} Q_i\overrightarrow{x_i}, for\ u_*^i \geq u_c \\ 0, for\ u_*^i < u_c \end{cases} \tag{4}$$

where $Q_i = Q\ (u_* = u_*^i)$ using Eqs. (1)–(3).

According to each saturated sand flux vector, $\overrightarrow{Q_i}$, the average sand flux, also referred to as the drift potential (*DP*), can be estimated for a flat erodible bed:

$$DP = \frac{\sum_{i=2}^{N_{obs}} \overrightarrow{Q_i}(t_i - t_{i-1})}{\sum_{i=2}^{N_{obs}}(t_i - t_{i-1})} \tag{5}$$

This quantity does not consider the directionality of sand transport over an entire period (Simmons et al., 2007). Therefore, the calculation of the resultant drift potential (*RDP*) is important:

$$RDP = \frac{\sum_{i=2}^{N_{obs}} \overrightarrow{Q_i}(t_i - t_{i-1})}{\sum_{i=2}^{N_{obs}}(t_i - t_{i-1})} \tag{6}$$

The *RDP* is normal to the sum of all the individual flux vectors and is strongly dependent on the wind direction. As a dimensionless parameter, the *RDP/DP* ratio is an important indicator of changes in the wind regime (Pearce and Walker, 2005; Tsoar, 2005). *RDP/DP*→1 indicates that sediment transport tends to be unidirectional. *RDP/DP*→0 means that most conveying components cancel each other out.

According to each saturated sand flux vector, we estimate the average sand flux of a flat erodible bed, which is used to represent the drift potential (*DP*). Sand flux is defined as the volume (or mass) of sand passing through a line of unit length perpendicular to the wind direction per unit time. Sometimes it is also noted as the dimensionless equivalent m^2/yr. Here, we follow the work of Courrech du Pont et al. (2014) and Gao et al. (2015). We consider that this definition of *DP* and *RDP* is more physical and has the physical unit.

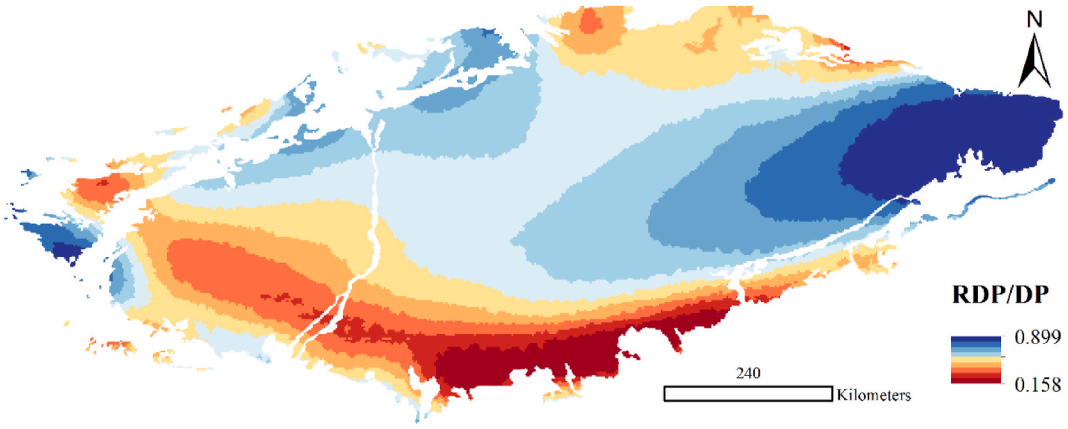

Fig. 8. Spatial pattern of the wind directional variability (*RDP/DP*) in the study area from 1979 to 2019. Based on the ERA5 wind data at a height of 10 *m*, the normal Kriging interpolation method is used to generate the continuous graph.

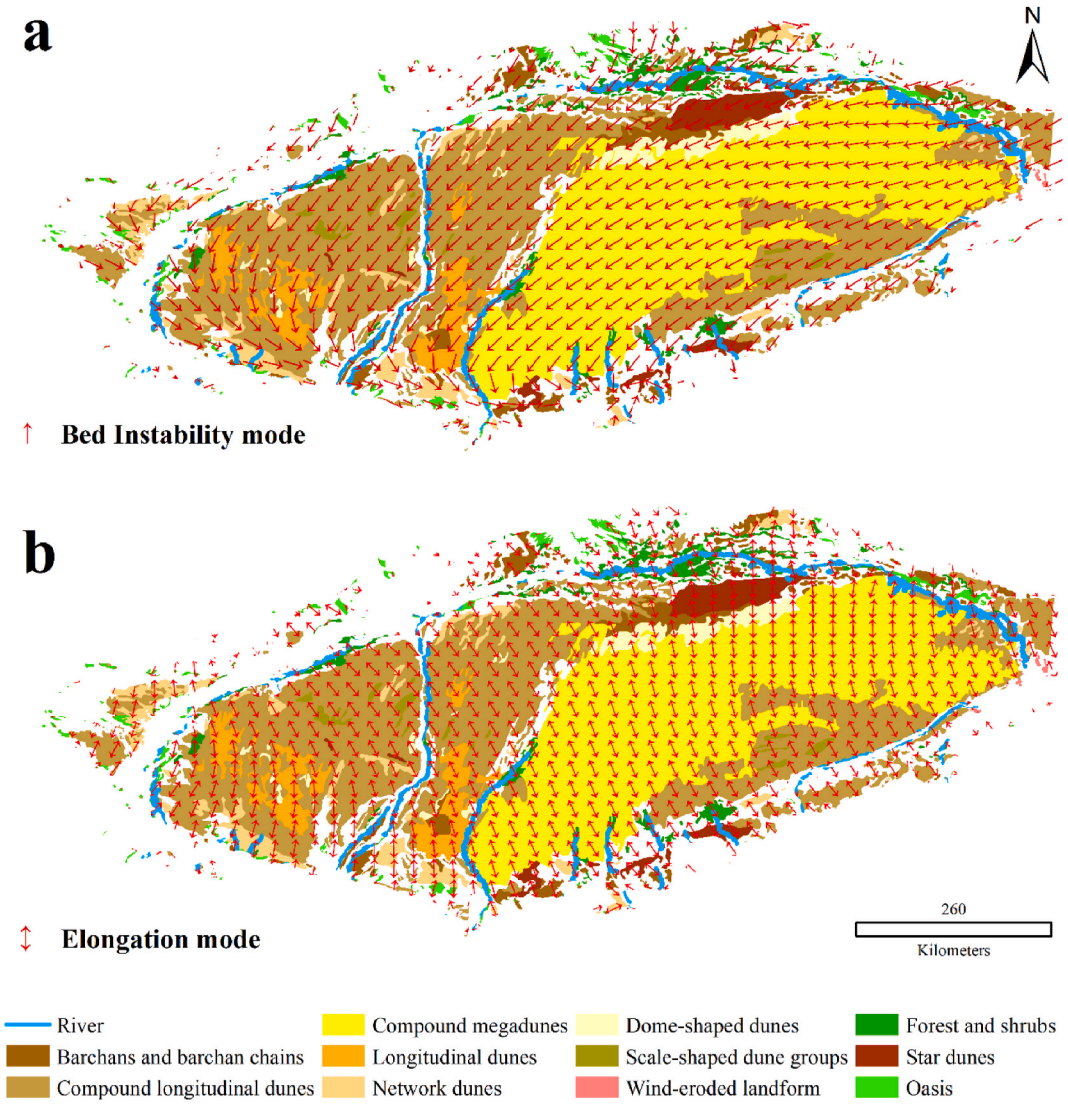

Fig. 9. Two modes of dune orientation in Taklamakan Desert. (a) Elongation mode and (b) bed instability mode. The modes were derived from the wind regime based on the ERA5 reanalysis assimilated dataset.

2.4. Two modes of dune orientation

Based on flume experiments and theoretical analyses, previous studies have proposed that there are two dune development modes according to varying sand supply quantities (Courrech du Pont et al., 2014). The direct manifestation is the difference in the dune orientation

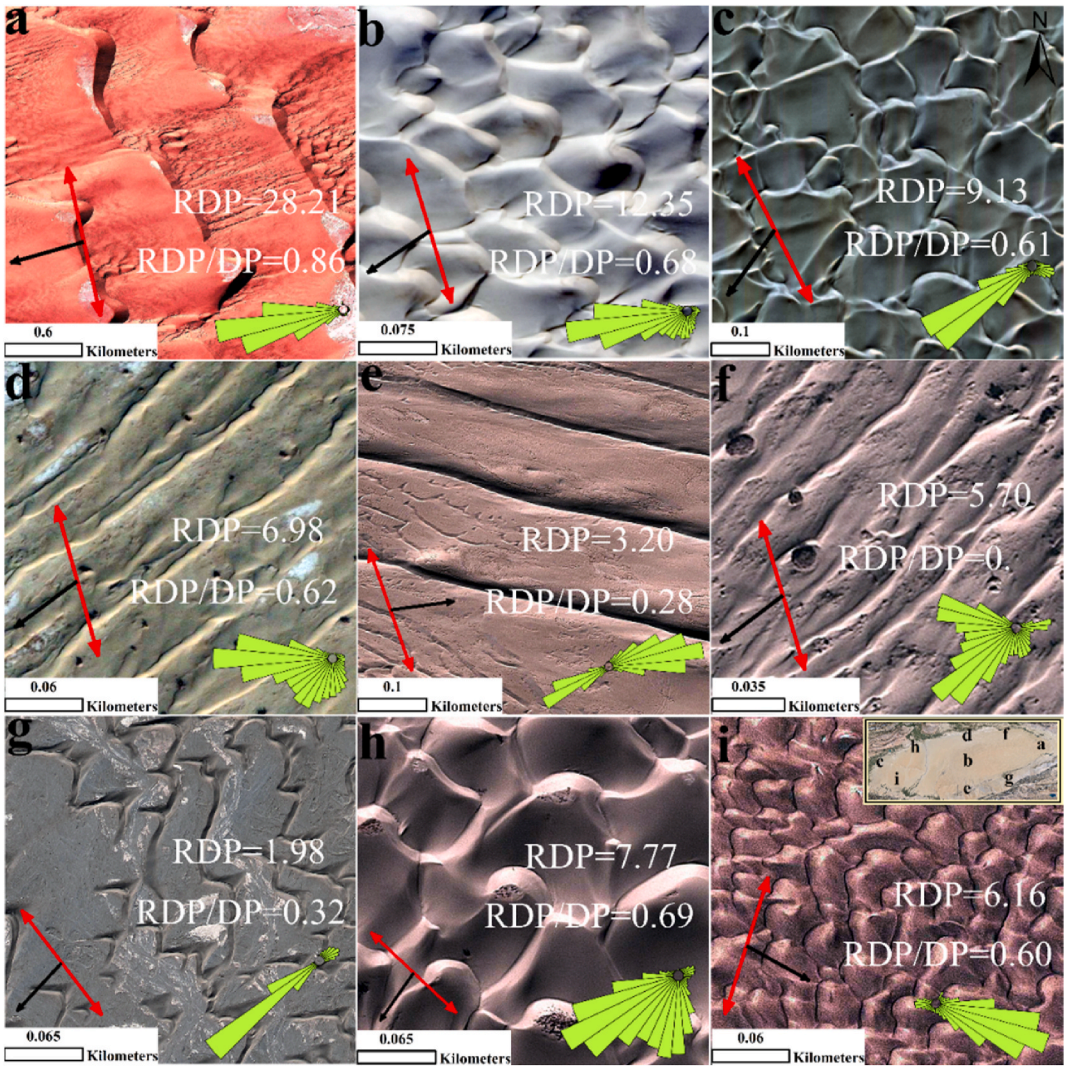

Fig. 10. The cases when the direction of sand transport corresponds well with the shape and strike of the dune. The green illustration represents the local sand flux roses; the red bi-directional and black one-directional arrows represent the bed instability and elongation modes, respectively. The resultant drift potential (*RDP*) represents the movement capacity of wind sand, while the *RDP/DP* (wind directional variability) ratio represents a change in the wind regime. (For interpretation of the references to colour in this figure legend, the reader is referred to the Web version of this article.)

and shape (Taniguchi et al., 2012; Parteli et al., 2014; Gao et al., 2015; Lü et al., 2017).

Under the action of a bi-directional wind, i.e., $\vec{W}_1$ and $\vec{W}_N$, the direction of a linear dune is α, the width is W, and the height is H (Fig. 5). The angles between the dunes and wind determine the actual sizes of the sand fluxes. The maximum value of the saturated sand flux $\vec{Q}_{sN}$, associated with the main wind, $\vec{W}_N$, is as follows:

$$\vec{Q}_{sN} = Q_0\left(1+\beta\frac{H}{L_N}\right)\vec{i} = Q_0\left(1+\beta\frac{H}{W}\left|\sin\alpha\right|\right)\vec{i}, \tag{7}$$

related to the wind, $\vec{W}_1$, as follows:

$$\vec{Q}_{s1} = \left[1+\beta\frac{H}{W}\left|\sin(\theta-\alpha)\right|\right]\left(\cos\theta\,\vec{i}+\sin\theta\,\vec{j}\right). \tag{8}$$

Owing to the correlation and interaction between dune shape and sediment transport, the direction of a dune determines the direction of the average aeolian sand transport throughout an entire period. With this effect and the constant aspect ratio, H/W, the direction can be obtained over time:

$$\langle\vec{Q}_s\rangle = \frac{1}{N+1}\left(N\vec{Q}_{sN}+\vec{Q}_{s1}\right) = \frac{Q_0}{N+1}\left\{\left[N(1+\gamma|\sin\alpha|)+\cos\theta(1+\gamma|\sin(\theta-\alpha)|)\right]\vec{i}+\sin\theta(1+\gamma|\sin(\theta-\alpha)|)\,\vec{j}\right\}, \tag{9}$$

where Q_0 is the value of saturated aeolian sand flow over a flat aeolian sand bed and β is the dimensionless coefficient for the wind speed. We also calculated the maximum value of the saturated sand flux, $\vec{Q}_{s1}$, where $\gamma = \beta H/W$. θ is the angle between the bi-directional wind. $\gamma = \beta H/W$ is a dimensionless topography parameter that accounts for the wind velocity increase from the flat sand bed to the sand dune crest (speed-up) (Jackson and Hunt, 1975). $\gamma = 0$ and $\gamma = +\infty$ represent that the wind

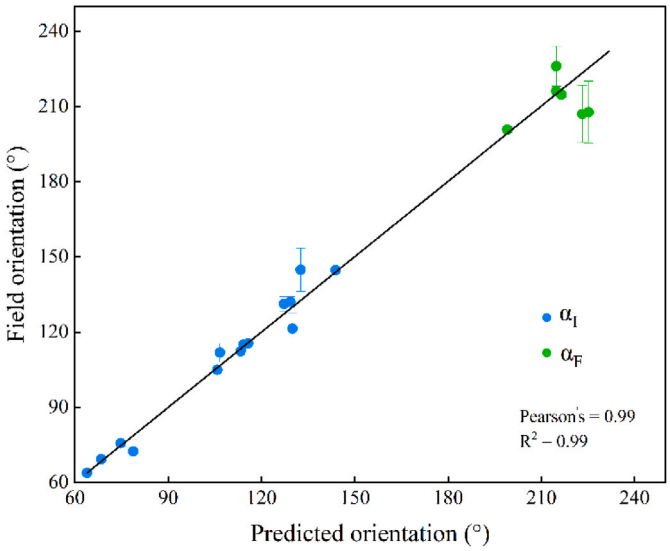

Fig. 11. Predicted versus observed dune orientation for the bed instability mode (α_I) and the elongation mode (α_F) in sand seas of Taklamakan Desert. The vertical error bars represent the standard deviation of the measurement.

velocity increase is 0 (i.e., there is no speed-up effect) and the wind velocity increase tends to be infinite (i.e., an extreme case, theory of existence). Usually, we use $\gamma = 1.6$ to study the dune orientation and sand transport (Gao et al., 2015). If $\gamma = 0$, the dune orientation of elongation mode is the same as *RDD*.

2.4.1. Bed instability mode

When the height and width of the dune remain unchanged, the average growth rate, σ, of the entire cycle is as follows:

$$\sigma \propto \frac{1}{H(N+1)}\left(\frac{Q_{s1}}{L_1}+N\frac{Q_{sN}}{L_N}\right) == \frac{Q_0}{(N+1)HW}\left[\left|\sin(\theta-\alpha)\right|+\gamma\sin^2(\theta-\alpha)+N\left|\sin\alpha\right|+N\gamma\sin^2\alpha\right] \tag{10}$$

where the growth rate, σ, is a function of the direction, α, of the dune. When the dune is large and can integrate multi-directional wind regimes, the actual direction of development is the direction with the highest growth rate (e.g., $d\sigma/d\alpha = 0$). In conclusion, the dune extension direction, α_I, maximizes sediment migration perpendicular to the top of the dune (Rubin and Hunter, 1987). If we consider that the aspect ratio does not change with time, the range of α_I, based on the value of coefficient γ, is therefore between:

$$\begin{cases} tan\alpha_I = -\dfrac{N+\cos\theta}{\sin\theta}, \ for\ \theta < \pi/2 \\ tan\alpha_I = \dfrac{N-\cos\theta}{\sin\theta}, \ for\ \theta \geqslant \pi/2 \end{cases}, \ when\ \gamma = 0 \tag{11}$$

which is when the flow is undisturbed. Equation (12) describes the solution when only considering an airflow disturbance caused by sand dunes:

$$\tan(2\alpha_I) = \frac{\sin(2\theta)}{\cos(2\theta)+N}, \ when\ \gamma = +\infty \tag{12}$$

2.4.2. Elongation mode

When a dune develops from a fixed sedimentary source and the angle, θ, between the main and secondary winds is $> \pi/2$, finger-like elongation of the dune can be observed. Therefore, if the sand source is fixed, the strike of the dune should be consistent with the resultant drift direction [Eq. (9)], forming an angle, α_F, with the main wind, $\overrightarrow{W}_N$, such that we obtain the following:

$$\tan\alpha_F = \frac{\sin\theta[1+\gamma\sin(\theta-\alpha_F)]}{N(1+\gamma\sin\alpha_F)+\cos\theta[1+\gamma\sin(\theta-\alpha_F)]} \tag{13}$$

The range of the dune direction α_F, varies with the value of γ:

$$\tan\alpha_F = \frac{\sin\theta}{N+\cos\theta}, \ \text{when}\ \ \gamma = 0 \tag{14}$$

$$\tan\alpha_F = \frac{\sin\theta}{\sqrt{N}+\cos\theta}, \ when\ \gamma = +\infty. \tag{15}$$

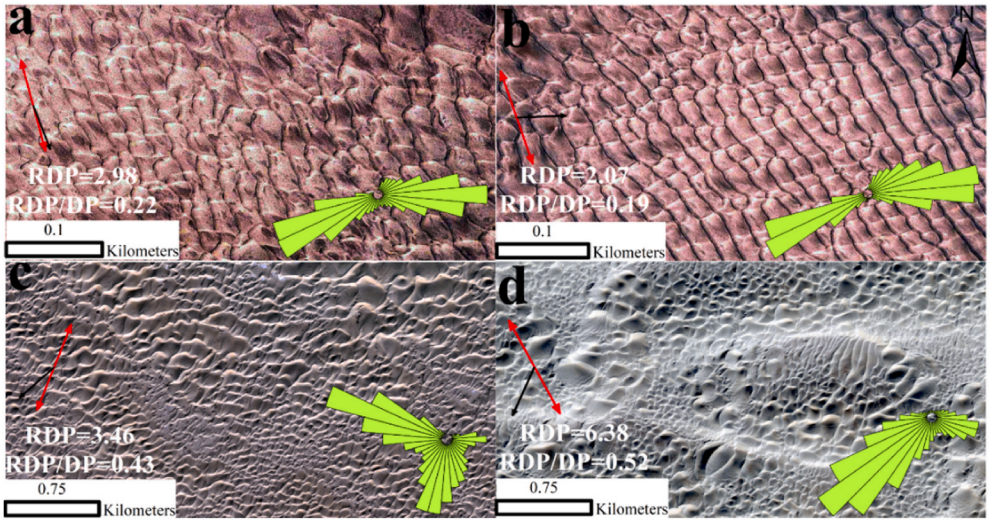

Fig. 12. The case when the direction of sand transport did not match well with the shape and strike of the dune. The green illustration represents the local sand flux roses; the red bi-directional and black one-directional arrows represent the bed instability and elongation modes, respectively. The resultant drift potential (*RDP*) represents the movement capacity of wind sand, while the *RDP/DP* (wind directional variability) ratio represents a change in the wind regime. (For interpretation of the references to colour in this figure legend, the reader is referred to the Web version of this article.)

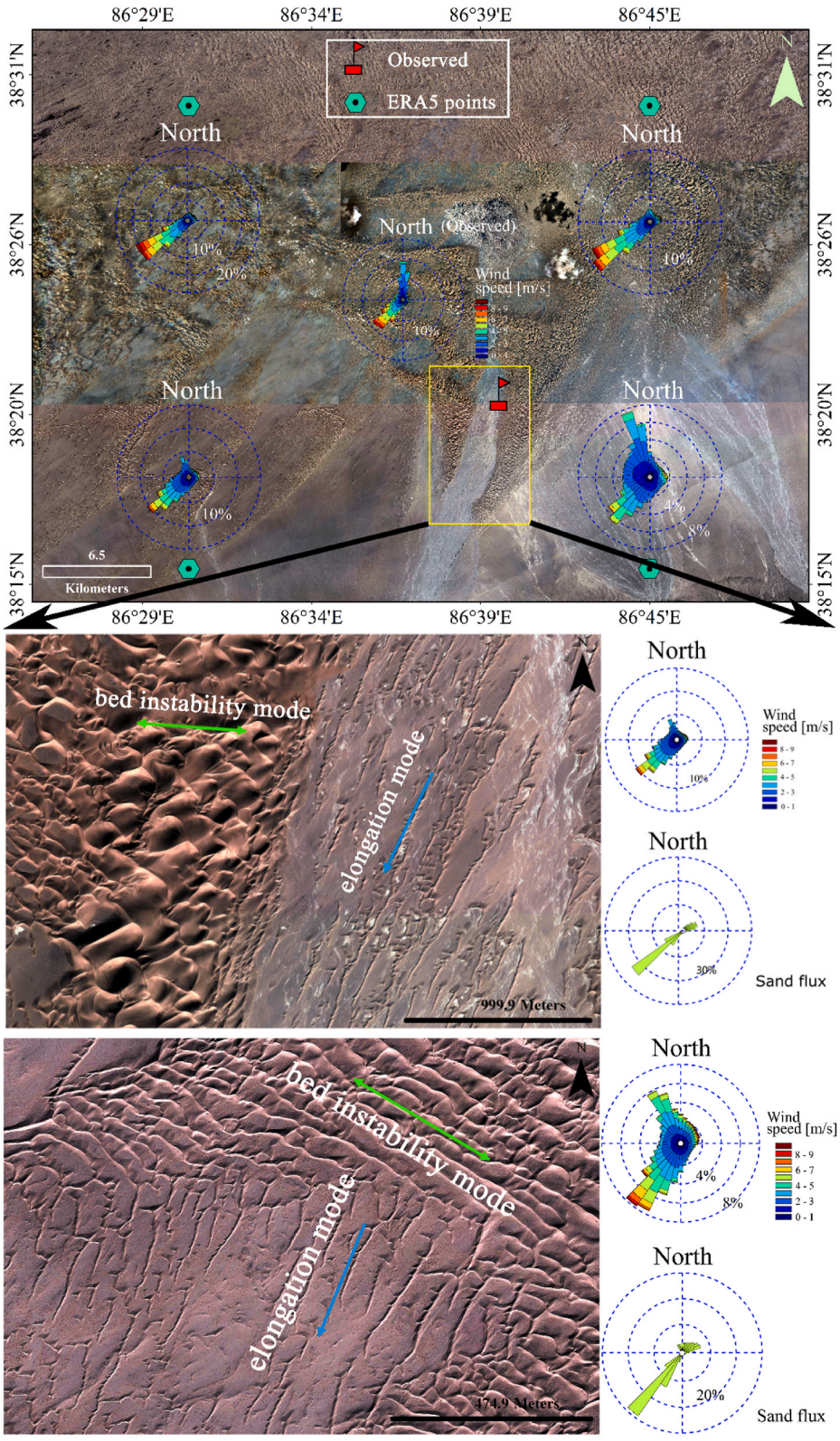

Fig. 13. Two modes of dune orientation under an identical wind regime. The green arrow represents the bed instability mode and the blue arrow represents the elongation mode. Wind roses indicate the strength and direction of the wind, while the sand flux roses indicate the direction of sand transport.

The solutions of Eqs. (14) and (15) are the dune orientation, α_F, in elongation mode.

Combined with the dune type classification, two dune growth mechanisms can be used to predict all dune types on Earth and other planetary bodies (Courrech du Pont et al., 2014; Gao et al., 2015; Lucas et al., 2014, 2015; Fernandez-Cascales et al., 2018; Rozier et al., 2019; Gadal et al., 2019, 2020). Two modes may locally coexist as a result of changes in sand availability or due to the development of superimposed bedforms. Gao et al. (2015) demonstrated a detailed study to investigate all simple dune types (from simple barchan dunes to pyramid dunes)

through numerical modelling based on two dune growth mechanisms, indicating that the two dune growth mechanisms can explain all dune types under any wind conditions (not only bi-directional regimes). Therefore, the two modes of dune orientation can be generalized to multidirectional wind regimes.

3. Results

3.1. Morphological characteristics of sand dunes

Taklamakan Desert, as the largest desert in China, contains almost all types of dunes (Fig. 6). We divided the Taklamakan Desert into eastern and western regions using the Keriya River as a boundary. East of the Keriya River, from the north to the south, almost all dune types are present. According to the classification criteria of Mckee (1979), there are simple barchan dunes and barchan chains (Wang et al., 2002) in desert areas along the northern edge, as well as some large compound domed dunes. The dune types that occupy most of the eastern Keriya River are large complex/compound mega dunes that extend east to west to the Keriya River. Among them, compound transverse dunes are the main dunes. The southern part of the desert belongs to the alluvial-diluvial plain on the Northern Slope of Kunlun Mountains, and the main geomorphic type is the Gobi. A small amount of shrub vegetation developed around seasonal rivers derived from the Kunlun Mountains. Influenced by unimodal northeasterly winds, barchan dunes and barchan dune chains are mainly developed in the southeastern margin of the desert. Asymmetrical barchan dunes can also be observed under the influence of regional wind systems. Compound linear dunes are also present. Along the southern edge of the desert, it moved to the southwest, and the influence of the northwest wind gradually became stronger. With the complexity of the wind regime, the dune types were mainly pyramid dunes (star dunes) and reversing dunes.

West of the Keriya River, a large number of compound longitudinal dunes are present in the areas. The desert to the west of the Hotan River is divided into two parts, north and south, with Mazatag Mountain, Gudong Mountain and Rostag Mountain as the boundary. North of the mountain range, complex/compound longitudinal dunes dominate, but on the windward slope of the mountain range, complex dunes such as pyramid dunes (star dunes) develop in abundance. However, the lee slope of the mountains extends to the southwest of the desert. Influenced by the northwest wind crossing the Pamir Plateau, the types of dunes are relatively rich, mainly consisting of compound longitudinal dunes and longitudinal dunes. The landscape of network dunes and linear dune symbiosis is developed in the southwest margin of the desert. Longitudinal dunes, which are particularly prominent, are mainly distributed in the south of the mountains, especially between the Hotan and Keriya rivers.

3.2. Wind regime and DP

3.2.1. DP distribution

Numerous factors, among which the wind regime is one of the most important, affect sand dune formation and development (Bagnold, 1941; Pye and Tsoar, 1990; Lancaster, 1995).

We refer to the global map of standard *DP* by Yizhaq et al. (2020) and find the same trend as our calculated results. The results of ERA5 data show that *DP* in the desert is relatively high. In this study, the *DP* and *RDP* of the entire Taklamakan Desert were calculated using ERA5 reanalysis wind data. As shown in Fig. 7, the entire Taklamakan Desert lies in a low wind energy environment, where the *DP* is significantly larger in the eastern part of the desert at the wind gap; the *DP* and *RDP* gradually decrease from the northeast to the southwest. Wind erosion in the eastern part of the Taklamakan Desert is very strong if the erosivity is expressed as drift potential by Wang et al. (2007).

3.2.2. Distribution of wind directional variability

The *RDP/DP*-value is a non-dimensional parameter that is often used to characterize the directional variability of the wind regimes. Wind direction variability is an important index reflecting wind regimes and a measure of wind direction. If the ratio of *RDP/DP* is larger, the wind direction variability is smaller, indicating that the wind direction is unimodal. The smaller the *RDP/DP* ratio is, the greater the wind direction variability is, indicating that the wind direction is more complex and changeable. This quantitative measure can be compared with synthetic landforms. On a macroscopic scale, the *RDP/DP* decreased from the east to the west (Fig. 8).

There is a small wind directional variability in the eastern part of the desert, which corresponds to a larger *RDP* with a single wind direction, dominated by northeasterly winds. A large *RDP/DP* ratio also exists near Ingisha County in the southwestern part of the desert, dominated by northwesterly unidirectional winds. South of the Mazatag and Rostag mountains and in the southern region of the desert, the *RDP/DP* ratio is small and the winds are complex, originating from all directions, corresponding to a smaller *RDP*.

3.2.3. Dune orientation

Dunes in two different directions can develop under a single multidirectional wind regime (Courrech du Pont et al., 2014). Two different patterns of dune development were identified based on the wind regime and sand availability (Fig. 9). When the sand source is abundant, the dunes mainly grow taller; the direction of the dunes is the direction that achieves maximum vertical resultant drift direction, corresponding to the bed instability mode of dune development (Fig. 9b). The east, southeast and south transverse dunes in the Taklamakan Desert have a general northwest-southeast trend, which is in better agreement with our calculated bed instability mode. The transverse dunes east of the Keriya River and the secondary transverse dunes developed on the longitudinal dunes west of the Keriya River can also be predicted by the bed instability mode.

When sand is scarce and for non-erodible beds, dunes develop and extend in the direction of resultant drift direction, corresponding to the elongation mode of sand dune development (Fig. 9a). In the desert region west of Hotan River, bounded by Mazatag Mountain, the longitudinal dunes in the north trend from northeast to southwest, and the longitudinal dunes in the south trend from northwest to southeast under the influence of northwest wind. A large number of the compound and complex longitudinal dunes developed in the west of the Keriya River and southwestern regions of the desert, which is more consistent with our calculated elongation mode, matching the overall resultant drift direction. Including in the southeastern part of the desert, linear dunes developed under unimodal wind regimes can also be matched with elongation mode.

3.3. Dune alignment predictions for dunes in the field

Using satellite images in combination with our calculated sand rose and the two dune development modes, we effectively predicted the orientation of some simple dunes (Fig. 10), such as barchan dunes that develop in areas with scarce sand sources and a single wind direction (Bagnold, 1941; Fryberger and Dean, 1979), and transverse dunes that gradually develop with increasing sources of sand. Barchan dune chains and transverse dunes match the bed instability mode, while linear dunes match the elongation mode, indicating that the orientation of linear dunes involves the scarcity of sand sources. Taking typical dunes in various directions of the desert as an example, 40 years of ERA5 wind data can well predict modern dune morphology in the desert.

Two modes are quantitatively compared to all field data in Fig. 11, suggesting that the 40 yr data of modern winds used to predict dune orientation provide an accurate picture of the wind regimes that built these sand seas in the past.

However, due to the influence of various factors, such as geological

time, topographic relief, vegetation cover, rivers and so on, the shape and direction of sand dunes in some areas of the desert cannot be well explained (Fig. 12).

4. Discussion

4.1. Coexistence of two dune orientation modes under the same wind regime

Elongation mode means that dunes grow by extension away from the source in the direction of the resultant sand flux at the crest, usually indicating the dune elongation direction. Bed instability mode means dunes grow in height and migrate selecting an orientation that maximizes the normal to crest components of transport, referring to the ability for a flat sand bed to organize in periodic bedforms as soon as there is sediment transport. Therefore, the same wind regime can lead to two dune orientations based on the sand availability. According to the Google satellite images, we located the areas where the two dune development modes occurred under the same wind regime (Courrech du Pont et al., 2014). According to the wind rose diagram of four ERA5 data points around the study area and the weather station data in the study area, we can confirm that the two modes develop under the same wind regimes. In other regions of the desert, the two modes exist in superposition. Courrech du Pont et al. (2014), based on flume experiments, showed that dunes with two different directions can form under a single multi-directional wind regime, with a nearly vertical direction along the sand ridgeline. Gao et al. (2015), based on numerical simulations, concluded that this situation results from an abundance or scarcity of sand sources, i.e., the availability of sand. In the bed instability mode, the erodible sand bed provided unlimited sand availability and the direction of resultant drift direction was nearly perpendicular to the wind direction, thus allowing for the development of more transverse dunes. However, in the longitudinal extension mode, the unerodable sand bed limited the availability of sand and the direction of resultant drift direction aligned with the wind direction, forming semi-developed linear dunes (Courrech du Pont et al., 2014). This is consistent with the morphology and strike of the dunes observed in the field (Fig. 13).

4.2. Wind regime interpretation over past 40 years for modern dunes

Understanding the characteristics of the near-surface wind regime is of great significance for studies on dune morphology and strike. The zonal general circulation model controls the near-surface wind regime in the Taklamakan Desert, with the influences of the topography and underlying surface (Zu et al., 2008). Owing to limitations associated with the meteorological stations in the desert, we used the ERA5 reanalysis wind data at a height of 10 *m*, which covers the entire desert, to calculate the near-surface wind regime. We found that the wind regime characteristics of most areas can explain the shape and direction of large modern sand dunes and several smaller sand dunes. For example, owing to the influence of northeastern winds in the eastern and southeastern regions of the desert, barchan dune chains and transverse dunes mostly occur in areas with abundant sand sources. Linear and asymmetric barchan dunes, extending along the southwest, mostly occur in areas near the edge of the desert, with scarce sand sources. The northern and middle regions of the desert are also affected by the northeastern wind, with the development of complex longitudinal or transverse dunes. These transverse and longitudinal dunes, which tend to occur in a superposition, occupy much of the Taklamakan Desert. However, in the southwest region of the desert, the northwestern wind dominates the complex longitudinal dunes. The modern wind field over the past 40 years can only explain the morphology and trend of modern sand dunes. Of course, for the regions where the wind regime has not changed over a large time scale, our prediction can also be matched with large dunes that have been formed for a long time.

5. Conclusions

A computational study of the wind regimes and sand transport in the Taklamakan Desert over the past 40 years revealed that the entire desert is mainly controlled by northeastern and northwestern wind systems. The wind regimes correspond well with the orientation and morphology of modern dunes. The southern part of the desert lies in the convergence of northwest and northeast winds, so wind conditions are more complicated (wind variability is mostly less than 0.3). Barchan dune chains and transverse dunes occur in the eastern and southeastern regions, where sand sources are abundant and influenced by a single northeasterly wind (wind direction variability is higher than 0.8). The development of dunes is mainly the increase in height and lateral extension. This is dominantly controlled by the bed instability mode. Moreover, the extension direction is almost perpendicular to the main wind direction. However, along the southeastern edge of the desert, many linear dunes and compound longitudinal dunes develop, mainly influenced by sand sources; they have developed on the non-erodible bed surface, with a scarce sand supply. The dune orientation is roughly aligned with the resultant drift direction and is mainly controlled by the elongation mode. Combined with the predicted results and sand transport distribution, we believe that the two modes can effectively explain the morphology and trend of most dunes, especially simple dunes. However, some dune geomorphology is not well interpreted by ERA5 wind data due to the influence of various factors, such as mountains, rivers, etc.

The ERA5 reanalysis data can effectively explain the morphology and orientation of modern dunes in the Taklamakan Desert. At a macro scale, most of the transverse and longitudinal dune trends in the Taklamakan Desert can also be well explained by ERA5 data. Although these large dunes formed in much longer periods. However, the simulation results may deviate from the actual dune orientation owing to the influence of subsurface conditions or topography in a specific area. The use of standardized macro data such as ERA5 reanalysis data to study wind and sediment transport in the Taklamakan Desert is innovative. The relationship between wind regime and dune formation and development is of great significance to the study of aeolian geomorphology and the prevention and control of aeolian disasters in the Taklamakan Desert.

CRediT authorship contribution statement

Wentao Sun: conceived the study, Formal analysis, interpreted the findings. **Xin Gao:** prepared the manuscript under mentorship from.

Declaration of competing interest

The authors declare that they have no known competing financial interests or personal relationships that could have appeared to influence the work reported in this paper.

Data availability

No data was used for the research described in the article.

Acknowledgments

This study was supported by the National Natural Science Foundation of China (No. 41971017 and 41861144020) and the High-level Talent Cultivation Project from the Xinjiang Institute of Ecology and Geography, Chinese Academy of Sciences (No. E0500201).

References

Andreotti, B., 2004. A two-species model of aeolian sand transport. J. Fluid Mech. 510, 47–70.

Bagnold, R.A., 1941. The Physics of Blown Sand and Desert Dunes. Springer, Netherlands.
Bristow, C.S., Bailey, S.D., Lancaster, N., 2000. The sedimentary structure of linear sand dunes. Nature 406 (1), 56–59.
Charru, F., Andreotti, B., Claudin, P., 2014. Sand ripples and dunes. Annu. Rev. Fluid Mech. 45 (1), 469–493.
Chen, W., Dong, Z., Yang, Z., Han, Z., Zhang, J., Zhang, M., 1995. Threshold velocities of sand-driving wind in Taklamakan Desert. Acta Geograph. Sin. 1995 (04), 360–367.
Courrech du Pont, S., Narteau, C., Gao, X., 2014. Two modes for dune orientation. Geology 42 (09), 743–746.
Dong, Z., Wang, X., Chen, G., 2000. Monitoring sand dune advance in the Taklamakan Desert. Geomorphology 35 (3–4), 219–231.
Dong, Z., Qian, G., Luo, W., et al., 2009. Geomorphological hierarchies for complex mega-dunes and their implications for mega-dune evolution in the Badain Jaran Desert. Geomorphology 106 (3–4), 180–185.
Durán, O., Herrmann, H., 2006. Modelling of saturated sand flux. J. Stat. Mech. - Theory Exp. 2006 (07). P07011–P07011.
Durán, O., Claudin, P., Andreotti, B., 2011. On aeolian transport: grain-scale interactions, dynamical mechanisms and scaling laws. Aeolian Res. 3 (3), 243–270.
Fernandez-Cascales, L., Lucas, A., Rodriguez, S., Gao, X., Spiga, A., Narteau, C., 2018. First quanti_cation of relationship between dune orientation and sediment availability, Olympia Undae, Mars. Earth Planet Sci. Lett. 489, 241–250.
Fryberger, S.G., Dean, G., 1979. Dune Forms and Wind Regime. In: A Study of Global Sand Seas, 1052. US Government Printing Office Washington, pp. 137–169.
Gadal, C., Narteau, C., du Pont, S.C., Rozier, O., Claudin, P., 2019. Incipient bedforms in a bidirectional wind regime. J. Fluid Mech. 862, 490–516.
Gadal, C., Narteau, C., Courrech du Pont, S., Rozier, O., Claudin, P., 2020. Periodicity in fields of elongating dunes. Geology 48 (4), 343–347.
Gao, X., Narteau, C., Rozier, O., Courrech du Pont, S., 2015. Phase diagram of dune shape and orientation depending on sand availability. Sci. Rep. 5, 14677.
Gunatilaka, A., Mwango, S., 1989. Flow separation and the internal structure of shadow dunes. Sediment. Geol. 61 (1–2), 125–134.
Hesp, P.A., 1981. The formation of shadow dunes. J. Sediment Petrol. 51 (1), 101–111.
Hesp, P.A., Smyth, T.A., 2017. Nebkha flow dynamics and shadow dune formation. Geomorphology 282, 27–38.
Hunter, R.E., Richmond, B.M., Alpha, T.R., 1983. Storm-controlled oblique dunes of the Oregon coast. Geol. Soc. Am. Bull. 94 (12), 1450–1465.
Iversen, J.D., Rasmussen, K.R., 1999. The effect of wind speed and bed slope on sand transport. Sedimentology 46 (4), 723–731.
Jackson and Hunt, 1975. Turbulent wind flow over a low hill. Qu. J. Royal Meteorol. Soc. 101 (430), 929–955.
Lancaster, N., 1995. Geomorphology of Desert Dunes. Routledge.
Lancaster, N., 2010. Assessing dune-forming winds on planetary surfaces-application of the gross bedform normal concept. LPI Contrib. 1552, 39–40.
Lettau, K., Lettau, H., 1978. Experimental and micrometeorological field studies of dune migration. In: Lettau, K., Lettau, H. (Eds.), Exploring the World's Driest Climate. University of Wisconsin Press, Madison, pp. 110–147.
Liu, X., Kang, Y., Chen, H., Lu, H., 2022. Comparison of surface wind speed and wind speed profiles in the Taklimakan Desert. PeerJ 10, e13001.
Livingstone, I., Warren, A., 1996. Aeolian Geomorphology. Addison–Wesley, Harlow, UK.
Lü, P., Narteau, C., Dong, Z., Rozier, O., Courrech du Pont, S., 2017. Unravelling raked linear dunes to explain the coexistence of bedforms in complex dune fields. Nat. Commun. 8, 14239.
Lucas, A., Rodriguez, S., Narteau, C., Charnay, B., Pont, S.C., Tokano, T., 2014. Growth mechanisms and dune orientation on Titan. Geophys. Res. Lett. 41 (17), 6093–6100.
Lucas, A., Narteau, C., Rodriguez, S., Rozier, O., Callot, Y., Garcia, A., Courrech du Pont, S., 2015. Sediment flux from the morphodynamics of elongating linear dunes. Geology 43 (11), 1027–1030.
Mckee, E.D., 1979. A Study of Global Sand Seas. U.S. Geological Survey Professional Paper.
McKee, E.D., 1982. Sedimentary structures in dunes of the Namib Desert, south west Africa. GSA (Geol. Soc. Am.) Spec. Pap. (Reg. Stud.) 188, 1–2.
Meng, X., Guo, J., Han, Y., 2018. Preliminarily assessment of ERA5 reanalysis data. J. Marine Meteorology 38 (1), 91–99.
Mottola, S., Arnold, G., Grothues, H.G., Jaumann, R., Michaelis, H., Neukum, G., et al., 2015. The structure of the regolith on 67P/Churyumov-Gerasimenko from ROLIS descent imaging. Science 349 (6247), aab0232.
Olauson, Jon, 2018. Era5: the new champion of wind power modelling? Renew. Energy 126, 322–331.
Owen, P.R., 1964. Saltation of uniform grains in air. J. Fluid Mech. 20 (02), 225.
Pähtz, T., Durán, O., Klerk, D.D., Govender, I., Trulsson, M., 2019. Local rheology relation with variable yield stress ratio across dry, wet, dense, and dilute granular flows. Phys. Rev. Lett. 123 (4), 048001.
Parteli, E.J., Duran, O., Bourke, M.C., Tsoar, H., Pöschel, T., Herrmann, H., 2014. Origins of barchan dune asymmetry: insights from numerical simulations. Aeolian Res. 12, 121–133.
Pearce, K.I., Walker, I.J., 2005. Frequency and magnitude biases in the 'Fryberger' model, with implications for characterizing geomorphically effective winds. Geomorphology 68 (1–2), 39–55.
Ping, L., Narteau, C., Dong, Z., Zhang, Z., Courrech du Pont, S., 2014. Emergence of oblique dunes in a landscape-scale experiment. Nat. Geosci. 7, 99–103.
Pye, K., Tsoar, H., 1990. Aeolian Sand and Sand Dunes. Springer, Netherlands, p. 416.
Rozier, O., Narteau, C., Gadal, C., Claudin, P., Courrech du Pont, S., 2019. Elongation and stability of a linear dune. Geophys. Res. Lett. 46 (781), 14521–14530.
Rubin, D.M., 2012. A unifying model for planform straightness of ripples and dunes in air and water. Earth Sci. Rev. 113 (3), 176–185.
Rubin, D.M., Hunter, R.E., 1987. Bedform alignment in directionally varying flows. Science 237 (4812), 276–278.
Sherman, D.J., Li, B., 2012. Predicting aeolian sand transport rates: a reevaluation of modes. Aeolian Res. 3 (4), 371–378.
Simmons, A., Uppala, S., Dee, D., Kobayashi, S., 2007. ERA-Interim: new ECMWF reanalysis products from 1989 onwards. ECMWF Newsletter 110, 25–35.
Sørensen, M., 2004. On the rate of aeolian sand transport. Geomorphology 59 (1–4), 53–62.
Sun, J., Zhang, Z., Zhang, L., 2009. New evidence on the age of the Taklamakan Desert. Geology 37 (2), 159–162.
Taniguchi, K., Endo, N., Sekiguchi, H., 2012. The effect of periodic changes in wind direction on the deformation and morphology of isolated sand dunes based on flume experiments and field data from the Western Sahara. Geomorphology 179, 286–299.
Tsoar, H., 1984. The formation of seif dunes from barchans-A discussion. Zeitschrift Fur Geomorphologie 28 (1), 99–103.
Tsoar, H., 2005. Sand dunes mobility and stability in relation to climate. Phys. Stat. Mech. Appl. 357 (1), 50–56.
Ungar, J.E., Haff, P.K., 1987. Steady state saltation in air. Sedimentology 34 (2), 289–299.
Wang, X., Dong, Z., Zhang, J., et al., 2004. Formation of the complex linear dunes in the central Taklimakan Sand Sea, China. Earth Surf. Process. Landf. 29 (6), 677–686.
Wang, X.M., Dong, Z.B., Zhang, J.W., Chen, G.T., 2002. Geomorphology of sand dunes in the Northeast Taklimakan Desert. Geomorphology 42 (3–4), 183–195.
Wang, X., Eerdun, H., Zhou, Z., Liu, X., 2007. Significance of variations in the wind energy environment over the past 50 years with respect to dune activity and desertification in arid and semiarid northern China. Geomorphology 86 (3–4), 252–266.
Wang, P., Zhang, J., Dun, H., Herrmann, H.J., Huang, N., 2020. Aeolian Creep Transport: Theory and Experiment. Geophys. Res. Lett. 47 (15).
Wasson, R., Hyde, R., 1983. Facts determining desert dune types. Nature 304, 337–339.
Werner, B.T., Kocurek, G., 1997. Bed-form dynamics: does the tail wag the dog? Geology 25 (9), 771–774.
Xiao, J., Qu, J., Yao, Z., Pang, Y., Zhang, K., 2015. Morphology and formation mechanism of sand shadow dunes on the Qinghai-Tibet Plateau. J. Arid Land 7 (1), 10–26.
Yang, Y., Liu, L., Shi, P., Zhao, M., Dai, J., Lyu, Y., Zhang, G., Zuo, X., Jia, Q., Liu, Y., Liu, Y., 2019. Converging effects of shrubs on shadow dune formation and sand trapping. J. Geophys. Res. Earth Surf. 124 (7), 1835–1853.
Yizhaq, H., Xu, Z., Ashkenazy, Y., 2020. The effect of wind speed averaging time on the calculation of sand drift potential: new scaling laws. Earth Planet. Sci. Lett. 544, 116373.
Zhang, D., Narteau, C., Rozier, O., Courrech du Pont, S., 2012. Morphology and dynamics of star dunes from numerical modelling. Nat. Geosci. 5 (7), 463–467.
Zhao, Y., Gao, X., Lei, J., Li, S., Cai, D., Song, Q., 2019. Effects of Wind Velocity and Nebkha Geometry on Shadow Dune Formation. J. Geophys. Res. Earth Surf. 124 (11), 2579–2601.
Zhao, Y., Gao, X., Lei, J., Li, S., 2021. Field measurements of turbulent flow structures over a nebkha. Geomorphology 375, 107555.
Zhou, C., Yang, F., Mamtimin, A., Huo, W., Yang, X., 2020. Wind erosion events at different wind speed levels in the Tarim Basin. Geomorphology 369 (1), 107386.
Zhu, Z., 1964. Movement patterns of sand dunes nearby oasis at southwestern margins of Taklamakan Desert. Acta Geograph. Sin. 30 (1), 35–50.
Zhu, Z., 1980. The General Induction to Chinese Desert. Science Press, Beijing, China, p. 107.
Zu, R., Xian, X., Qiang, M., Yang, B., Qu, J., Zhang, K., 2008. Characteristics of near-surface wind regimes in the Taklamakan Desert, China. Geomorphology 96 (1–2), 39–47.